

A survivin-driven, tumor-activatable minicircle system for prostate cancer theranostics

TianDuo Wang,^{1,4} Yuanxin Chen,⁴ David Goodale,⁵ Alison L. Allan,^{2,3,5,6} and John A. Ronald^{1,4,6}

¹Department of Medical Biophysics, Schulich School of Medicine & Dentistry, Western University, London, ON N6A 5B7, Canada; ²Department of Anatomy & Cell Biology, Schulich School of Medicine & Dentistry, Western University, London, ON N6A 5B7, Canada; ³Department of Oncology, Schulich School of Medicine & Dentistry, Western University, London, ON N6A 5B7, Canada; ⁴Robarts Research Institute – Imaging Research Laboratories, London, ON N6A 3K7, Canada; ⁵London Regional Cancer Program, London Health Science Centre, London, ON N6C 2R5, Canada; ⁶Lawson Health Research Institute, London, ON N6C 2R5, Canada

Gene vectors regulated by tumor-specific promoters to express transgenes specifically in cancer cells are an emerging approach for cancer diagnosis and treatment. Minicircles are shortened plasmids stripped of prokaryotic sequences that have potency and safety characteristics beneficial for clinical translation. Previously, we developed minicircles driven by the tumor-specific survivin promoter, which exhibits elevated transcriptional activity in aggressive cancers, to express a secreted reporter for blood-based cancer detection. Here we present the first activatable, cancer theranostic minicircle system featuring a pair of diagnostic and therapeutic minicircles expressing *Gaussia* luciferase for urine-based cancer detection or cytosine deaminase:uracil phosphoribosyltransferase for gene-directed enzyme prodrug therapy. Diagnostic minicircles revealed urinary reporter output related to cellular survivin levels. Notably, mice with aggressive prostate tumors exhibited significantly higher urine reporter activity than mice with non-aggressive tumors and healthy mice after intratumoral minicircle administration. Therapeutic minicircles displayed specific cytotoxicity in survivin-rich cancer cells and significantly attenuated growth of aggressive orthotopic prostate tumors in mice. Use of these minicircles together creates a theranostic system that can first identify individuals carrying aggressive prostate cancer via a urinary test, followed by stringent control of tumor progression in stratified individuals who carry high-risk prostate lesions.

INTRODUCTION

Gene transfer—introduction of foreign genetic material into cells—is a promising avenue for novel cancer therapeutics and diagnostics. By creating gene vectors driven by tumor-specific promoters to selectively activate transgene expression in cancer cells but not healthy cells, off-target effects can be minimized.¹ Historically, these “tumor-activatable” vectors have predominantly encoded therapeutic transgenes for cancer gene therapy.^{2–5} More recently, researchers have also created tumor-activatable vectors encoding secreted and/or imaging reporters as a means to detect cancer.^{6–8} Naturally, encoding reporter and therapeutic genes extends these systems into the field of theranostics.⁹

Among the numerous discovered tumor-specific promoters, the survivin promoter (pSurvivin) is a promising candidate. Also known as

baculoviral inhibitor of apoptosis repeat-containing 5 (BIRC5), survivin has been studied widely as a cancer biomarker because of its near-exclusive presence in cancer cells but not healthy adult tissue.^{10–12} These characteristics have allowed groups to leverage the tumor-specific activity of pSurvivin to drive activatable transgene expression in prostate,¹³ breast,¹⁴ and liver cancer,¹⁵ among others. Furthermore, survivin is elevated in many aggressive metastatic tumors compared with non-aggressive tumors,^{16,17} which could lead to higher transgene expression in relevant tumors.

Despite continued refinement, the goal of developing a highly efficient and safe tumor-activatable vector has yet to be fully realized. The majority of tumor-activatable vectors developed so far have used viral vectors or non-viral plasmid constructs. Viral vectors have been the most popular because of their relatively high gene transfer efficiency compared with plasmids.¹⁸ However, factors such as random genomic integration and unwanted immune responses have raised major concerns regarding safety,^{19–21} leading many to posit that plasmid-based strategies may be safer for widespread clinical use.²² The main challenges recombinant plasmids face are inefficient delivery, fast clearance, and transfer of antibiotic resistance genes to host microbiota.^{23,24} The goal of addressing the limitations of plasmids motivated the inception of minicircle (MC) vectors, which are smaller plasmid derivatives stripped of their prokaryotic backbone.²⁵ Removal of the backbone confers greater transfection efficiency with MCs compared with plasmids through a reduction in vector size. Additionally, MCs have prolonged expression profiles compared with plasmids because the plasmid backbone is a common target for transcriptional silencing.^{26,27} Thus, tumor-activatable MCs could overcome the limitations of plasmids by achieving higher transfer efficiency into cancer cells and inducing more robust transgene expression while eliminating prokaryotic components that could otherwise compromise clinical safety and translation.

Received 15 August 2020; accepted 13 January 2021;
<https://doi.org/10.1016/j.omto.2021.01.007>.

Correspondence: John A. Ronald, Robarts Research Institute – Imaging Research Laboratories, 1151 Richmond Street, North London, ON N6A 3K7, Canada.
E-mail: jronald@robarts.ca



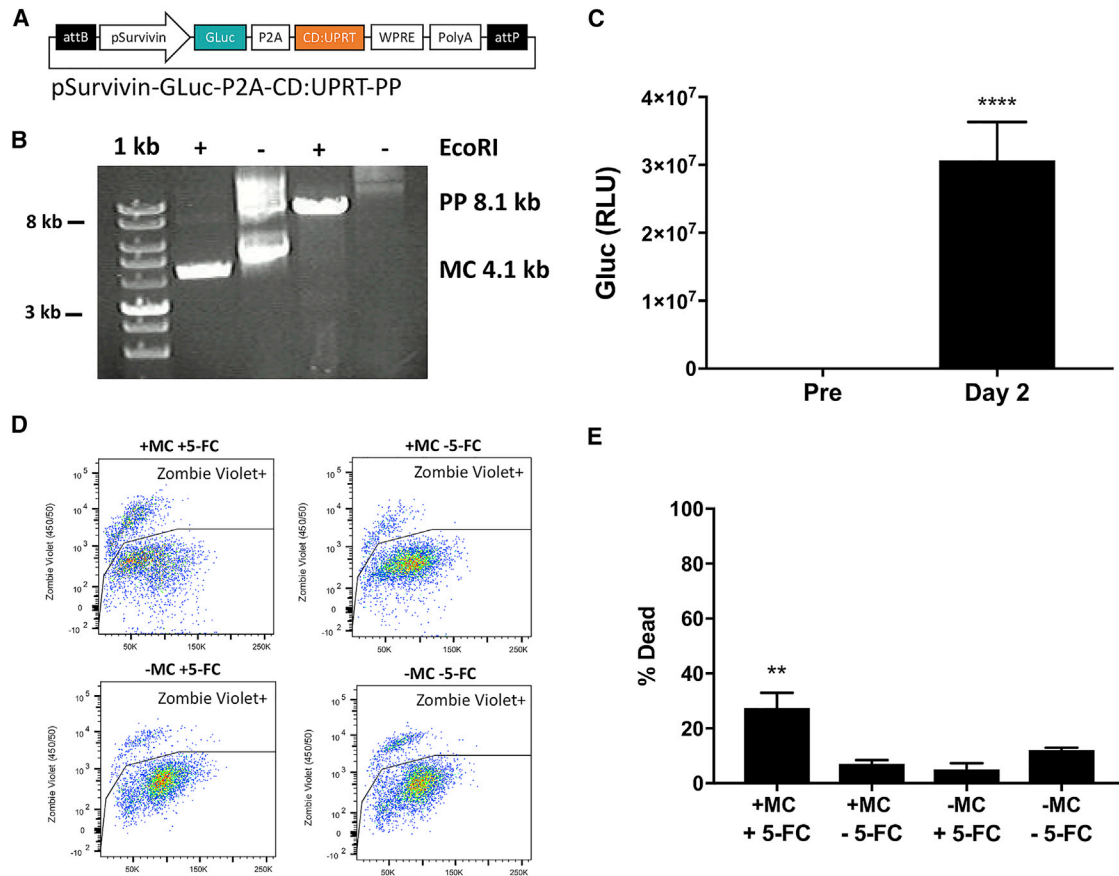


Figure 1. Characterization of theranostic MCs *in vitro*

(A and B) Vector map of the pSurv-GLuc-CD:UPRT-PP expression cassette (A) with agarose gel electrophoresis (B) to confirm proper production of the PP (8.1 kb) and MC (4.1 kb). (C) GLuc activity in cell supernatant before and on day 2 after transfection with pSurv-GLuc-CD:UPRT-MCs (n = 5). (D and E) Flow cytometry plots of PC3MLN4 cells on day 5 post-transfection stained with the Zombie Violet Cell Fixable Viability Kit (D) with quantification (E) of Zombie Violet+ (dead) cells (n = 3). Data are presented as mean \pm SD (****p < 0.001, **p < 0.01).

Our group previously developed the first tumor-activatable MC system that used pSurvivin to drive expression of a secreted reporter gene for cancer detection.²⁸ MCs complexed with linear polyethylenimine (PEI) reliably distinguished mice with melanoma lung tumors from tumor-free mice through a blood test. Recently, we also demonstrated the utility of these MCs for discerning human prostate cancer xenografts of varying aggressiveness.²⁹ Because of the inherent modularity of MCs, here we explore use of tumor-activatable MCs for cancer theranostics. Specifically, we built and validated a pair of novel survivin-driven MCs, which we called diagnostic MCs and therapeutic MCs, that can be used separately or together for urine-based cancer detection and gene-directed enzyme prodrug therapy (GDEPT).³⁰ Diagnostic MCs encode *Gaussia* luciferase (GLuc), a secreted reporter gene isolated from the marine copepod *Gaussia princeps* that is primarily cleared via the renal pathway and detectable in urine.³¹ Therapeutic MCs expressed the fusion enzyme cytosine deaminase:uracil phosphoribosyltransferase (CD:UPRT).³² CD:UPRT catalyzes conversion of the non-toxic prodrug 5-fluorocytosine (5-FC) to the anti-tumor metabolites 5-fluo-

rouracil (5-FU) and 5-FU monophosphate (5-FUMP), leading to inhibition of cancer proliferation through thymidine deprivation.³³ Importantly, CD:UPRT has been used previously in preclinical models for treating several types of cancer, including prostate cancer.³⁴ Here we demonstrate the complementarity of diagnostic MCs for detection of aggressive, high-survivin orthotopic prostate tumors in mice via increased urine GLuc activity, with therapeutic MCs encoding CD:UPRT to attenuate the growth of high-survivin prostate tumors.

RESULTS

In vitro evaluation of all-in-one MCs co-expressing reporter and therapeutic genes

As the first step toward establishing a tumor-activatable theranostic MC system, we co-encoded GLuc and CD:UPRT transgenes on a single survivin-driven construct to create an “all-in-one” parental plasmid (PP) (pSurvivin-GLuc-P2A-CD:UPRT-PP, 8.1 kb; Figure 1A) and subsequent all-in-one theranostic MCs (4.1 kb). Proper MC production was confirmed by gel electrophoresis (Figure 1B). All-in-one

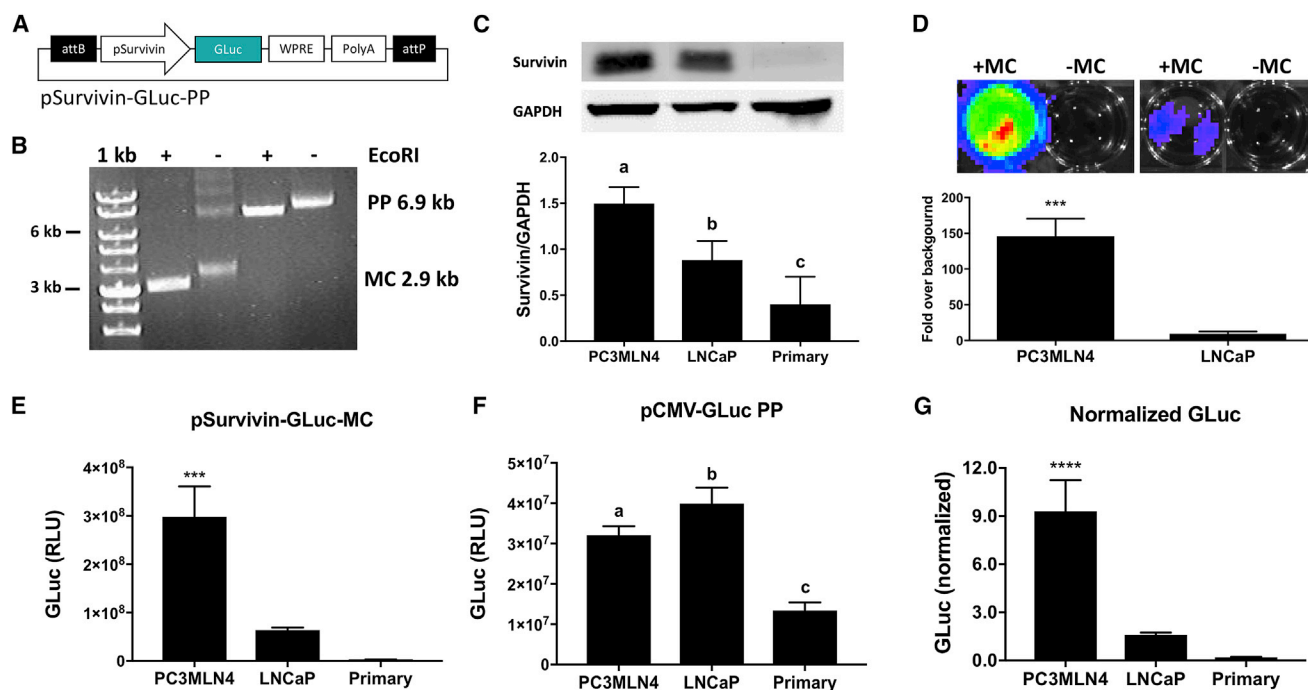


Figure 2. Characterization of secreted reporter expression *in vitro*

(A and B) Vector map of the pSurv-GLuc-PP expression cassette (A) with agarose gel electrophoresis (B) to confirm proper production of the PP (6.9 kb) and MC (2.9 kb). (C) Western blot for cellular survivin expression in PCa and primary prostate epithelial cells ($n = 3$). Band intensities were quantified using ImageJ and are shown relative to GAPDH. (D) GLuc bioluminescence signal above background from PCa cells transfected with pSurv-GLuc-MCs ($n = 5$). (E–G) GLuc activity in supernatant from cell lines transfected with (E) pSurv-GLuc-MCs or (F) pCMV-GLuc plasmids on day 2 post-transfection with (G) normalized values ($n = 3$). (H) Groups designated by different letters are significantly different ($p < 0.05$). Data are presented as mean \pm SD (**** $p < 0.001$, *** $p < 0.005$).

MCs were complexed with PEI and transfected into PC3MLN4 cells, which we have shown previously to express a high level of survivin.²⁹ Prior to transfection, no appreciable levels of GLuc activity were found in medium, but significantly greater GLuc activity above baseline was detected 2 days post-transfection (Figure 1C). To evaluate therapeutic effect, the percentage of dead cells was determined in transfected or naive cells with or without 5-FC treatment using flow cytometry of Zombie Violet-stained cells. This revealed that $27.4\% \pm 4.5\%$ of cells were dead 4 days after they were transfected with all-in-one MCs and treated with 5-FC, which was significantly higher compared with all other conditions, which were not significantly different from each other.

Diagnostic MCs induce GLuc activity related to cellular survivin levels

Although all-in-one MCs showed potential as a theranostic agent in survivin-rich prostate cancer (PCa) cells, we posited that a system composed of two smaller MCs encoding GLuc and CD:UPRT separately would improve transfection efficiency and transgene expression, potentially leading to increased diagnostic and therapeutic efficacy. We first engineered diagnostic PPs (pSurvivin-GLuc-PP, 6.9 kb) and successfully produced diagnostic MCs (2.9 kb; Figures 2A and 2B). Equimolar amounts of MCs and their PP counterparts were transfected into PC3MLN4 cells, and after

2 days, MCs produced significantly higher GLuc activity in culture medium than PPs (Figure S1). Compared with all-in-one MCs (Figure 1B), diagnostic MCs displayed increased GLuc activity at similar time points. We also used bioluminescence imaging (BLI) to visualize intracellular GLuc activity from diagnostic MCs across PCa cells with varying survivin levels (Figure 2C). Two days post-transfection, PC3MLN4 cells exhibited a significantly higher (>100-fold) signal above background than LNCaP cells (~10-fold; Figure 2D), indicative of significantly greater GLuc expression in PC3MLN4 (high-survivin) cells compared with LNCaP (low-survivin) cells. To evaluate GLuc secretion, 2 days post-transfection, GLuc activity in culture medium was significantly higher in PC3MLN4 cells compared with LNCaP and primary prostate epithelial cells (Figure 2E). No significant difference in GLuc activity between LNCaP and primary prostate cells was found. To account for variable transfection efficiency across cell types, cells were also transfected with constitutively on pCMV-GLuc plasmids. Comparable GLuc activity between PC3MLN4 and LNCaP cells was found, whereas primary prostate cells exhibited significantly lower (~60%) GLuc activity (Figure 2F). GLuc activity values obtained using the pCMV-GLuc plasmids were used to normalize GLuc values obtained with pSurvivin-GLuc-MCs (Figure 2G). Following normalization, PC3MLN4 cells maintained significantly higher GLuc activity values compared

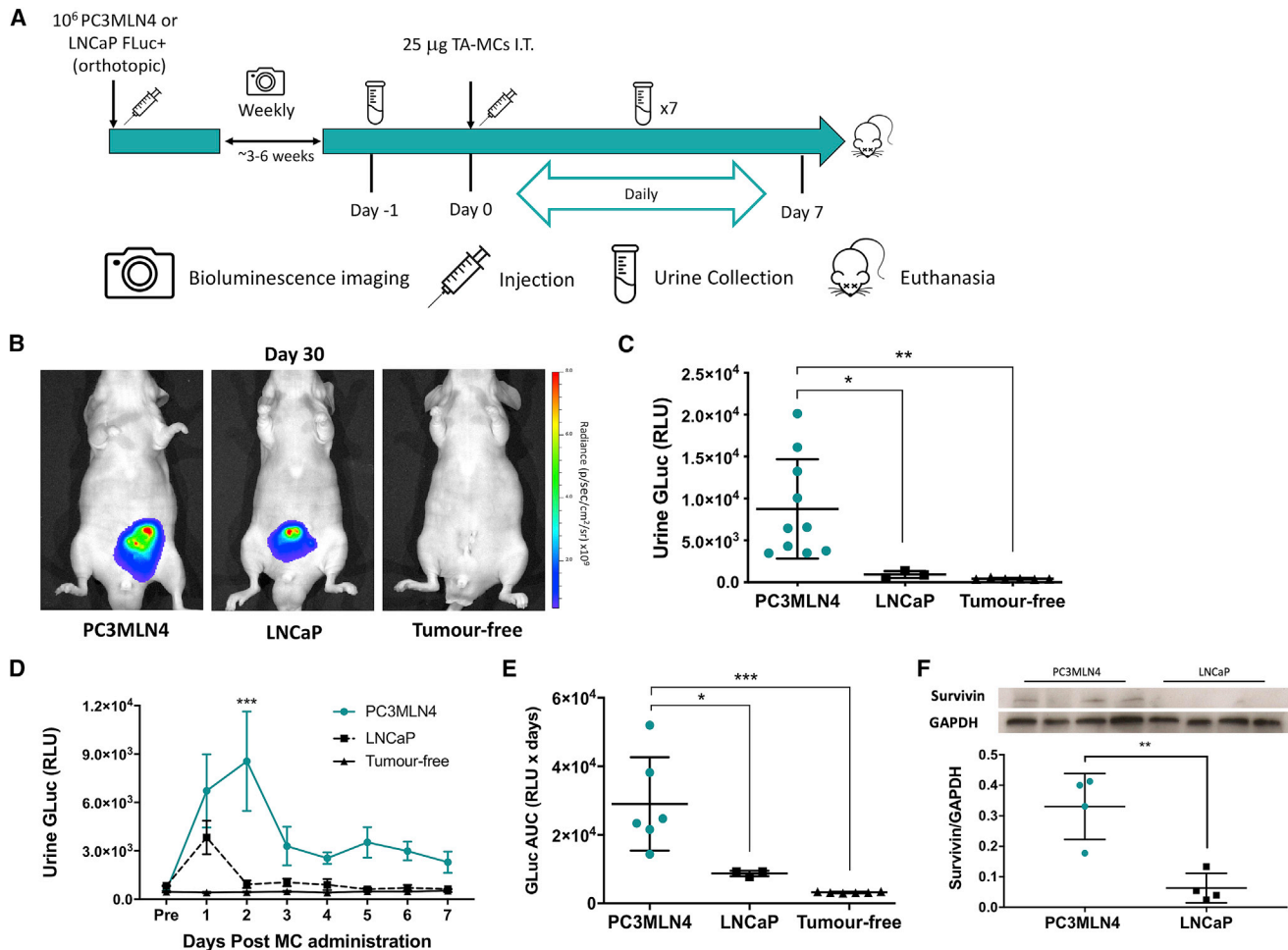


Figure 3. Evaluation of urine GLuc activity in nude mice with orthotopic prostate tumors

(A) Timeline of intratumoral administration of pSurv-GLuc tumour-activatable MCs (TA-MCs) and subsequent urine sampling. (B) Representative FLuc BLI images of mice 30 days after tumor implantation. (C) Urine GLuc activity on day 2 post-MC administration into PC3MLN4 (n = 10), LNCaP (n = 3), or no tumors (n = 6). (D and E) Daily urine GLuc activity in mice bearing PC3MLN4 (n = 6), LNCaP (n = 3), or no tumors (n = 6) (D) and AUC analysis (E) over 1 week post-MC administration of mice bearing PC3MLN4 (n = 6), LNCaP (n = 3), or no tumors (n = 6). (F) Western blot for survivin levels in tumor lysates (n = 4). Data are presented as mean \pm SD (**p < 0.005, **p < 0.01, *p < 0.05).

with LNCaP and primary prostate cells, reflective of the relative survivin levels across the cell types.

Diagnostic MCs identify mice carrying aggressive prostate tumors via increased urine GLuc activity

To first evaluate diagnostic MCs *in vivo*, we established PC3MLN4 FLuc+ subcutaneous tumors on the right flank of male nude mice and performed intratumoral injections with pSurvivin-GLuc-MCs (25 μ g). Urine was collected 1 day before and then on days 2, 5, and 7 after MC injection. In tumor-bearing mice, urine GLuc activity was increased significantly on all days post-MC injection (peaking on day 2) compared with GLuc activity pre-MC injection as well as at all time points following intramuscular MC injections (Figure S2). To assess diagnostic MCs across different tumor types, we established orthotopic PC3MLN4 FLuc+ and LNCaP FLuc+ prostate tumors, and a

linear correlation was found between FLuc BLI signal and viable cell number in these engineered cells (Figure S3). Because the same number of LNCaP cells displayed a roughly 6-fold lower BLI signal than PC3MLN4 cells, we adjusted the signal expected for LNCaP tumors accordingly when tracking tumor growth. When tumors reached ~ 150 mm³ (3–4 weeks for PC3MLN4, 5–6 weeks for LNCaP; Figure S4), diagnostic MCs (25 μ g) were injected intratumorally, and urine was collected 1 day prior to and daily after MC administration (Figure 3A). Prior to MC injection, all animals exhibited negligible GLuc activity in the urine. For mice carrying PC3MLN4 tumors, urine GLuc activity peaked on day 2, which was significantly higher compared with mice with LNCaP tumors and tumor-free mice at this same time point (Figure 3C). After day 2, GLuc activity in PC3MLN4 mice declined by $\sim 60\%$ compared with peak levels and remained at a steady low level until the endpoint (Figure 3D). In mice

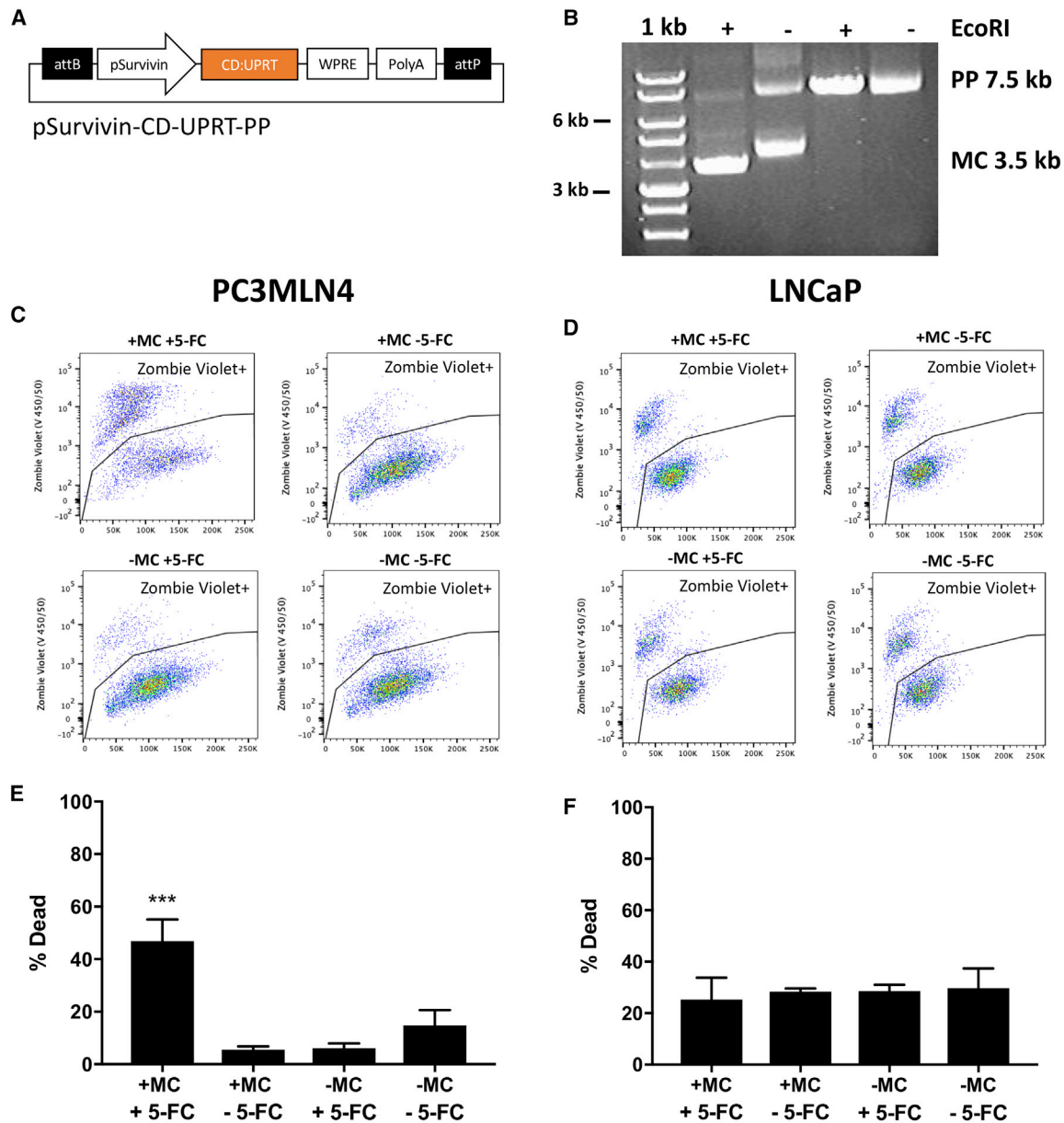


Figure 4. Characterization of the suicide gene therapy system in PCa cells with varying levels of survivin

(A and B) Vector map of the pSurv-CD:UPRT-PP expression cassette (A) with agarose gel electrophoresis to confirm proper production of the PP (7.5 kb) and MC (3.5 kb) (B). (C–F) Flow cytometry plot of (C) PC3MLN4 and LNCaP (D) cells on day 5 post-transfection stained with the Zombie Violet Cell Fixable Viability Kit with (E and F) quantification of Zombie Violet+ (dead) cells (n = 3). Data are presented as mean ± SD (***)p < 0.005).

carrying LNCaP tumors and tumor-free mice that received intraprostatic MC injections, urine GLuc activity post-MC injection was not significantly above baseline levels throughout the study. Area-under-curve (AUC) analysis of GLuc activity over time showed significantly higher AUC values in mice carrying PC3MLN4 tumors compared with other groups (Figure 3E). Endpoint western blot analysis of tumor tissue revealed significantly increased survivin levels in PC3MLN4 compared with LNCaP tumors (Figure 3F).

Therapeutic MCs are selectively cytotoxic in survivin-high prostate cancer cells

To evaluate the use of pSurvivin-driven MCs for therapy, we engineered pSurvivin-CD:UPRT-PPs (7.5 kb) and successfully produced therapeutic MCs (3.5 kb; Figures 4A and 4B). The therapeutic effect of pSurvivin-CD:UPRT-MCs was assessed using flow cytometry post-transfection. Zombie Violet staining revealed that 46.9% ± 6.9% of PC3MLN4 cells transfected and treated with 5-FC were

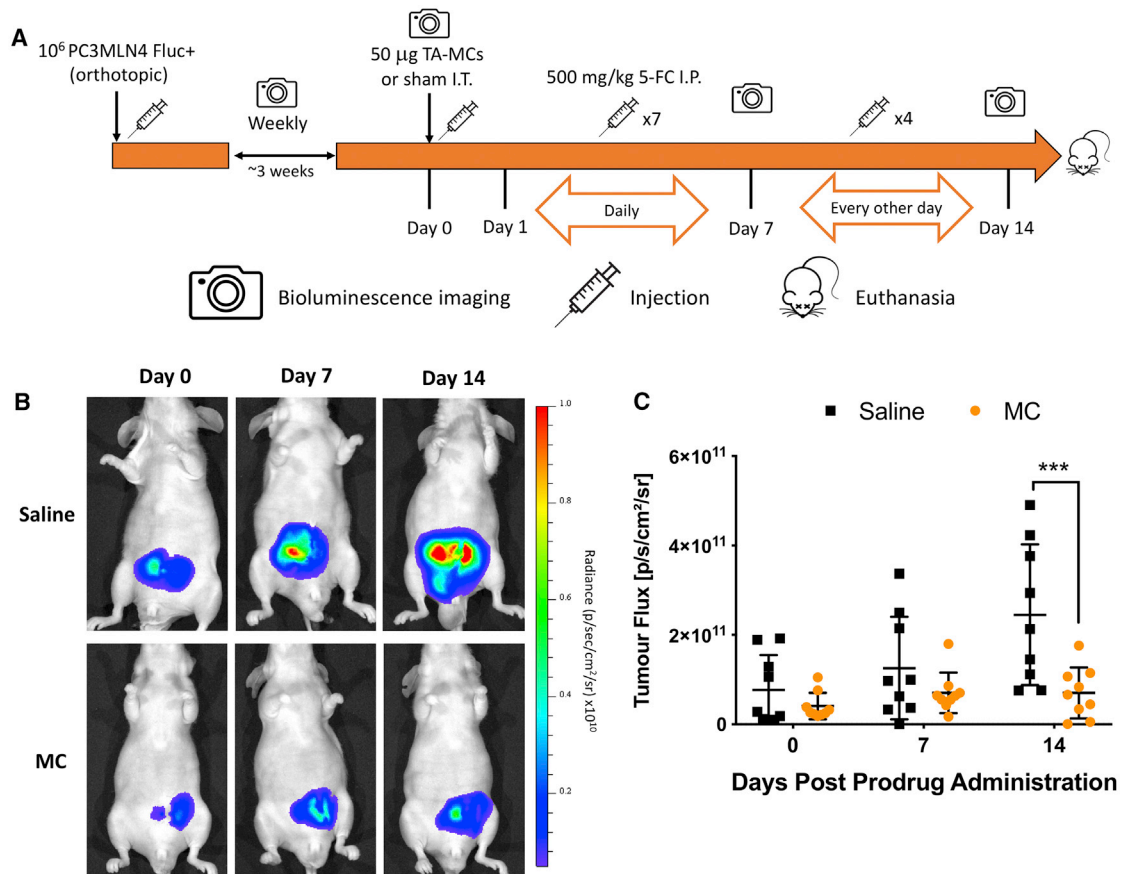


Figure 5. Assessment of the therapeutic effect in nude mice with high-survivin orthotopic prostate tumors

(A) Timeline of intratumoral administration of pSurv-CD:UPRT-MCs, 5-FC treatment, and BLI time points. (B and C) Representative FLuc BLI images (B) with quantification (C) from nude mice with PC3MLN4 FLuc+ tumors post-injection of intratumoral saline ($n = 9$) or pSurv-CD:UPRT-MCs until the endpoint at 14 days ($n = 9$). Data are presented as mean \pm SD (** $p < 0.005$).

dead, and this percentage was significantly higher than under all other conditions (Figures 4C and 4E). In contrast, no difference in the percentage of dead cells was found for LNCaP cells between all treatment groups (Figures 4D and 4F). These findings suggest that therapeutic MCs are selectively cytotoxic to PCa cells expressing high survivin levels when supplied with the prodrug 5-FC, although we hypothesize that cytotoxicity can be optimized by improving transfection efficiency and increasing the prodrug dosage. Based on these results, we further validated the observed effects of therapeutic MCs on PC3MLN4 FLuc+ cells by performing BLI to evaluate cell viability. Four days post-transfection and beyond, PC3MLN4 FLuc+ cells treated with 5-FC exhibited a significantly reduced BLI signal compared with all other conditions (Figures S5A and S5B).

Therapeutic MCs attenuated the growth of aggressive orthotopic prostate cancer

We next evaluated the effects of therapeutic MC administration on the growth of survivin-rich orthotopic PC3MLN4 FLuc+ tumors in nude mice. To mitigate discrepancies in initial tumor size between groups,

tumor burden was assessed weekly with BLI, and when the BLI signal reached $\sim 10^{11}$ p/s, therapeutic MCs (50 μ g) or saline was injected intratumorally. On the day of MC injection (day 0), the tumor BLI signal was not significantly different between groups (Figures 5B and 5C). Following MC or saline injections, mice were treated daily with 500 mg/kg 5-FC over 14 days (Figure 5A), and cancer cell viability was monitored over time with BLI. On average, saline-treated mice showed a significant 3.16-fold increase in BLI signal over the 14-day treatment period, whereas the BLI signal in mice receiving therapeutic MCs did not change significantly (Figure 5B and 5C). At the endpoint, mice that received therapeutic MCs exhibited a significantly lower tumor BLI signal than saline-treated mice.

DISCUSSION

Important characteristics for gene-based cancer technologies include sufficient expression from tumors to produce a detectable signal or therapeutic effect while presenting minimal expression of transgenes in normal tissues. Survivin-driven, tumor-activatable MCs are a promising platform for this purpose. Our initial work on this

technology described activatable MCs encoding secreted embryonic alkaline phosphatase (SEAP) for detection of lung melanoma tumors.²⁸ This system was then adapted for PCa, where mice carrying high-survivin, aggressive subcutaneous PCa tumors could be distinguished from low-survivin, non-aggressive tumors via a blood SEAP test.²⁹ Here we report our latest iteration of the tumor-activatable MCs by introducing urinary GLuc reporter tests for tumor detection and CD:UPRT-mediated GDEPT, describing the first activatable MC system for these purposes.

We first sought to improve blood-based diagnostic MCs by replacing SEAP with a bicistronic cassette encoding GLuc and CD:UPRT. Despite initial assessments with these all-in-one MCs showing potential for simultaneous theranostics, we found greater efficacy when each transgene was encoded separately on individual MCs. GLuc-expressing MCs produced reporter levels titrated to survivin expression in transfected cells. Notably, these diagnostic MCs exhibited markedly higher output than their PP counterparts, which can likely be attributed to increased transfection efficiency and an improved expression profile,²⁶ highlighting the value of MCs over plasmids in improving detection sensitivity. By measuring urine GLuc activity, diagnostic MCs injected intratumorally were able to specifically discern mice carrying aggressive, high-survivin PC3MLN4 prostate tumors from mice with low-survivin LNCaP tumors as well as healthy mice receiving intraprostatic MC injections. Because of the ease of sampling urine longitudinally, we were able to perform AUC analysis of urine GLuc activity measured daily over a week and found that mice carrying aggressive tumors displayed a significantly increased GLuc AUC compared with mice with LNCaP tumors and healthy mice. Estimating total GLuc output and assessing secretion kinetics over time may prove to be especially fruitful clinically because these diagnostic metrics may be more accurate than a single measurement.³⁵ GLuc-expressing MCs have several advantages over our original SEAP MCs. First, a urine-based test facilitates longitudinal study compared with blood-based tests because of the ease of urine collection. Second, the GLuc gene (~550 bp) is considerably shorter than SEAP (~1,500 bp), reducing overall MC size. Moreover, non-human-derived enzyme-based reporter genes, such as GLuc, offer the distinct advantage of being naturally absent from the human body and provide amplified readouts compared with measuring endogenous compounds—traits that could improve detection of smaller tumors for earlier diagnosis.³⁶ We also designed therapeutic MCs expressing CD:UPRT to be used in conjunction with our diagnostic MCs for treatment of GLuc-detected, survivin-high, aggressive tumors. Therapeutic MCs selectively limited the growth of high-survivin PC3MLN4 cells but not low-survivin LNCaP cells. Administered intratumorally, these therapeutic MCs attenuated the growth of aggressive prostate tumors over a 14-day period compared with sham-treated mice. We hypothesize that, by improving transfection efficiency and transgene expression, this therapeutic effect can be enhanced to eradicate aggressive tumors.

In this study, we chose PCa as our initial model to evaluate tumor-activatable MCs because of the unique diagnostic challenge PCa pre-

sents, which can be attributed to its high prevalence but varied lethality across individuals. PCa becomes lethal when it metastasizes outside of the prostate, and we envision using diagnostic MCs to stratify individuals with primary tumors into groups at high and low risk of future metastasis. This important prognostic information could improve patient-centered care and reduce overtreatment. Because of the transient nature of our episomal MCs, particularly in dividing cancer cells, GLuc will not be detectable in individuals for extended periods of time, potentially allowing repeated administration of GLuc-expressing MCs as a monitoring tool.³⁷ This synthetic reporter system may be used in conjunction with current diagnostic techniques like biopsy and prostate-specific antigen screening to improve disease management. When individuals with aggressive, high-risk PCa are identified, therapeutic MCs may be used sequentially to control cancer progression, and these MCs could even be delivered intraprostatically during a standard 12-core biopsy. Therapeutic MCs would act as an intermediate treatment post-diagnosis to prevent cancer spreading prior to individuals receiving more radical procedures such as prostatectomy or brachytherapy because these procedures are considerably more effective for early-stage disease.³⁸ A dual-MC theranostic system allows separate administration of MCs pre- and post-diagnosis to match their clinical use and maximize expression, whereas the same would not be possible for an all-in-one theranostic MC because both genes would be administered together. One potential alternative is to explore promoters such as astrocyte-elevated gene 1 (AEG-1)³⁹ or prostate-specific membrane antigen (PSMA),⁴⁰ among others, which have been used for prostate cancer-specific transgene expression. Beyond prostate cancer, our MC system may be readily expanded to a pan-cancer theranostic technology because survivin is highly expressed in many common cancers, including breast, lung, pancreatic, ovarian, colorectal, and liver cancer.⁴¹

Because of previous work showing that survivin expression correlates with increasing Gleason grade,¹⁶ pSurvivin was an attractive driver of transgene expression for our MCs. However, we also report some limitations of pSurvivin, such as low levels of transgene expression in healthy tissues and its weak activity compared with stronger, albeit constitutive, promoters. These drawbacks limit the sensitivity of our system, which could affect the viability of systemically delivered constructs in humans. One solution to increase transgene expression is to amplify pSurvivin activity using custom regulatory elements. For instance, the two-step transcriptional amplification (TSTA) system uses a GAL4-VP16 fusion protein and GAL4 DNA binding sites upstream of transgenes of interest to enhance tissue-specific expression from weaker promoters,^{42,43} and these TSTA elements have yet to be included in MCs. Inclusion of a scaffold/matrix attachment region (S/MAR) in the 5' untranslated region may also provide architectural anchors to promote replication of episomal gene vectors using host machinery.⁴⁴ S/MAR sequences have been shown to enhance and prolong MC expression in rapidly proliferating cells,⁴⁵ and further *in vivo* study could establish S/MAR as a way to strengthen MC expression. Another important diagnostic use of tumor-activatable MCs is delivery of imaging reporter genes. Several groups have explored tumor-activatable vectors encoding imaging reporter genes for cancer detection with imaging

modalities such as fluorescence,¹³ photoacoustics,⁴⁶ and positron emission tomography (PET).³⁹ Work using survivin-driven MCs to drive imaging reporter gene expression is ongoing in our group.

Many human clinical trials have utilized plasmid vectors to deliver transgenes.^{22,47} Beyond improved transfection rates compared with plasmids, MCs are more resistant to gene silencing because of fewer CpG motifs,⁴⁸ DNA shearing forces,⁴⁹ a higher supercoiled fraction,⁵⁰ and enhanced serum stability.⁵¹ To facilitate use in humans, a critical aspect to optimize is the MC-to-transfection agent ratio, and MCs allow a higher effective dose than plasmids because a given transfection agent amount will contain more moles of MCs than plasmids. Another important factor to consider for translation is delivery. To maximize local delivery of MCs in this study, we performed intratumoral injections into multiple tumor loci. Despite some concerns such as leakage and uneven distribution, intraprostatic injections have already been performed for treatment of chronic prostatitis and benign prostatic hyperplasia⁵² and in clinical trials with GDEPT for prostate cancer.⁵³ It would be valuable, nonetheless, to cultivate our system for systemic delivery. Our first work describing melanoma detection delivered SEAP-MCs intravenously and robustly identified mice bearing lung tumors by measuring blood SEAP activity.²⁸ The linear PEI agent we used here primarily delivers non-viral vectors to the lungs and liver, and so systemic delivery to the prostate can be improved by using targeted transfection agents and/or nanoparticles.^{54,55} Exploring technologies to provide robust tumor-specific systemic delivery of MCs is a major focus going forward.

In this study, we built and evaluated a novel theranostic system comprised of a pair of survivin-driven MCs for detection and treatment of aggressive prostate tumors. This system may serve as an effective way to identify individuals with prostate cancer with high-risk lesions and expedite treatment post-diagnosis with the hope to ultimately lessen the psychophysical burden of this terrible disease.

MATERIALS AND METHODS

PP and MC construction

A dual-transgene, tumor-activatable theranostic PP driven by pSurvivin and encoding GLuc and CD:UPRT separated by the P2A self-cleavage peptide sequence (pSurvivin-GLuc-P2A-CD:UPRT-PP) was designed in-house and built by Genscript (NJ, USA). Single-transgene pSurvivin-driven PPs were designed and built in-house using the In-Fusion HD Cloning Kit (Takara Bio, CA, USA). First, pSurvivin-SEAP-PP²⁸ was digested with AgeI and NheI, and the linearized backbone was isolated via gel extraction. To create pSurvivin-GLuc-PP, the GLuc2 transgene from pCMV-GLuc (New England Biolabs, MA, USA) was subcloned into the linearized backbone. To make pSurvivin-CD:UPRT-PP, the CD:UPRT gene from pSELECT-CD:UPRT (InvivoGen, CA, USA) was subcloned into the same linearized product. MCs were generated from their respective PP using a previously described production system.⁵⁶ Briefly, each PP was transformed into ZCY10P3S2T *E. coli*, and viable kanamycin-resistant colonies were selected and cultured at 37°C in lysogeny broth (LB) for 6 h followed by terrific broth (TB) for 12 h. To generate MCs

via site-specific recombination, induction of ϕ C31 integrase and Sce-I endonuclease was achieved through addition of an equal volume of LB containing 0.001% (v/v) L-arabinose and 4 mL 1 N NaOH and incubation for 5.5 h at 30°C. Production of PPs followed the same protocol without addition of arabinose. PPs and MCs were purified from *E. coli* using an endotoxin-free Maxi kit (QIAGEN, ON, Canada) and resuspended in nuclease-free water. MCs were cleaned to remove PP contamination using the Plasmid-Safe ATP Dependent DNase Kit (Epicenter, WI, USA), followed by the DNA Clean & Concentrator Kit (Zymo Research, CA, USA).

Cell culture and transduction

Human LNCaP PCa cell lines were obtained from the ATCC (VA, USA), and PC3MLN4 cells were a kind gift from Dr. Hon Leong (Western University, ON, Canada). Primary prostate epithelial cells were also obtained from the ATCC. LNCaP and PC3MLN4 cells were maintained in RPMI 1640 medium (Wisent Bioproducts, QC, Canada). Primary cells were grown in prostate epithelial cell basal medium (ATCC). All media were supplemented with 10% (v/v) fetal bovine serum (FBS) and 5% (v/v) antibiotic-antimycotic, and cells were cultured at 37°C in 5% CO₂. The absence of mycoplasma contamination was routinely verified using the MycoAlert Mycoplasma Detection Kit (Lonza, NY, USA). To generate cells that can be detected using bioluminescence imaging, PC3MLN4 and LNCaP naive cells were transduced with lentiviral vectors (in 8 μ g/mL Polybrene) encoding tdTomato (tdT) and firefly luciferase (FLuc) driven by the human elongation factor-1 alpha promoter (pEF1 α). Transduced cells were washed, and tdT-positive cells were sorted using a FACSAria III fluorescence-activated cell sorter (BD Biosciences, CA, USA).

In vitro assessment of diagnostic MCs

PCa and primary prostate epithelial cells were seeded at 5×10^4 cells/well in a 24-well plate 1 day prior to transfection. Cells were transfected with pSurvivin-GLuc-MCs (1 μ g) after complexation with 2 μ L of jetPEI, a linear PEI transfection agent (Polyplus Transfection, PA, USA). On day 2 post-transfection, 100 μ L of medium was collected from each well and centrifuged briefly, and the supernatant was stored at -20°C . Each time medium was collected, wells were washed with phosphate-buffered saline (PBS), and fresh medium was added; thus, the GLuc measurement reflected protein production over the desired time intervals. GLuc activity in samples was measured using the Bioluminescence Assay Kit (NEB, Ipswich, MA, USA). GLuc assay solution (50 μ L) was added to 20 μ L of each sample, and total luminescence over 5 s (expressed in relative light units [RLUs]) was measured using a Glomax 20/20 luminometer (Promega, WI, USA). Separately seeded cells were transfected with pCMV-GLuc plasmids (1 μ g, NEB), and GLuc activity was measured using the same kit. GLuc activity from pSurvivin-GLuc-MCs was normalized to GLuc activity from pCMV-GLuc plasmids. To compare expression from MCs with their PP counterparts, PC3MLN4 cells were seeded at 5×10^4 cells/well in a 24-well plate. One day later, cells were transfected with equimolar pSurvivin-GLuc-PPs (1 μ g) or pSurvivin-GLuc-MCs (0.42 μ g) complexed with jetPEI. To maintain the same mass of DNA and volume of jetPEI

between wells, pEF1 α -tdT-luc2-PPs (0.58 μ g) were co-transfected into cells receiving MCs. GLuc activity in medium samples was assessed as described above. To visualize intracellular GLuc activity, medium was removed from transfected cells and washed with D-PBS, and fresh medium was added prior to addition of 5 μ M h-coelenterazine to each well. Plates were then imaged on an IVIS Lumina XRMS scanner (PerkinElmer, MA, USA). Average radiance (p/s/cm²/sr) per well was quantified by placing regions of interest over each well using Living Image 4.5.2 software (PerkinElmer, MA, USA).

In vitro assessment of therapeutic MCs

To evaluate therapeutic MCs, PCa cells were seeded in 24-well plates and transfected with pSurvivin-CD:UPRT-MCs (1 μ g). Cells were transferred to 6-well plates 1 day later, and then cell medium was supplemented with 500 μ g/mL 5-FC (Sigma, MO, USA). For control conditions, pSurvivin-CD:UPRT-MCs and/or 5-FC in medium was withheld. Every other day, medium in wells was removed and replaced with fresh medium with 500 μ g/mL 5-FC. The percentage of dead cells was assessed using the Zombie Violet Fixable Viability Kit (BioLegend, CA, USA). Briefly, on day 5 post-transfection, cells were collected and resuspended in PBS containing 1:500 Zombie Violet dye. Following 15-min incubation in the dark, the percentage of dead cells (dye-positive cells at 405 nm) was determined using a FACSCanto flow cytometer (BD Biosciences). Flow cytometry results were analyzed using FlowJo v.10. To measure the viability of FLuc+ cells using BLI, the same steps of seeding, transfection, and passaging steps were used as above. FLuc BLI was done on days 0, 2, 4, 5, 6, and 7 on the IVIS scanner after addition of 150 μ g/mL D-luciferin to each well, and the average radiance (p/s/cm²/sr) for each well was measured. After each imaging session, wells were washed with PBS, and fresh medium containing 500 μ g/mL 5-FC was added.

In vitro assessment of theranostic MCs

To assess GLuc activity and cell death from PC3MLN4 cells transfected with dual-transgene pSurvivin-GLuc-P2A-CD:UPRT-MCs, the same procedures were used as described for diagnostic and therapeutic MCs.

Tumor models

All animal procedures were approved by the University Council on Animal Care at the University of Western Ontario (protocol 2015-058) and are in compliance with Canadian Council on Animal Care (CCAC) and Ontario Ministry of Agricultural, Food and Rural Affairs (OMAFRA) guidelines. For all animal work, 6- to 8-week-old male nu/nu athymic nude mice were used (Charles River Laboratories, QC, Canada). For subcutaneous tumor models (n = 5), one million PC3MLN4 cells were injected subcutaneously into the right flank of mice. Tumor volume was assessed using calipers, and MCs were injected intratumorally when tumors reached \sim 150 mm³. Tumor volume was calculated using the following formula⁵⁷: tumor volume = 0.5*(length \times width²). For orthotopic tumors models (n = 18), mice were anesthetized and maintained at 2% isoflurane, and a small incision (<1 cm) was made along the midline to expose the lower peritoneum. Gently lifting the bladder from the abdominal cavity toward the head, the prostate was located, and one million PC3MLN4 FLuc+

cells were injected into the right anterior prostate lobe. An identical procedure was performed using LNCaP FLuc+ cells mixed with an equal volume of Matrigel (VWR, ON, Canada) to aid tumor formation.⁵⁸ Incisions were closed with sutures and surgical staples, and mice were administered Metacam analgesic. BLI was performed weekly post-surgery on the IVIS scanner to assess FLuc+ tumor development, and tumors were injected intratumorally with MCs \sim 3–6 weeks post-surgery. As a rough estimate of tumor size, orthotopic PC3MLN4 tumor (n = 9) volumes were measured using calipers prior to MC injections, and tumor volume was correlated with BLI signal, which was measured 1 day prior to surgery. At the endpoint, animals were euthanized using an overdose of isoflurane followed by cervical dislocation. Tumor tissue was dissected and cut into two parts. One part was immersed in 4% paraformaldehyde (PFA) for 24 h at 4°C and then immersed in PBS at 4°C, and the second part was snap-frozen with liquid nitrogen and then stored at -80° C.

In vivo diagnostic MC assessment in subcutaneous and orthotopic tumors

Diagnostic MCs were prepared by combining pSurvivin-GLuc-MCs (25 μ g/mouse) with 3 μ L of *in vivo*-jetPEI (Polyplus Transfection) to achieve an N/P ratio of 8 (the N/P ratio describes the number of nitrogen residues in *in vivo*-jetPEI per nucleic acid phosphate). This MC-PEI complex was then resuspended in equal volumes of 10% (w/v) glucose and incubated at room temperature for 30 min. For subcutaneous PC3MLN4 tumors (n = 5), mice were anesthetized and maintained with 2% isoflurane, and then MC complexes were injected intratumorally into 3–4 loci. For intramuscular injections in healthy mice (n = 4), MC complexes were injected directly into the right flank. For these animals, urine was collected 1 day before and on days 2, 5, and 7 after MC injection. Urine collection was done by placing individual mice into small sterile boxes, and each mouse was monitored every 5 min for urination. Urine samples (\sim 50–100 μ L/mouse) were pipetted into a microcentrifuge tube and stored at -20° C until assayed. Urine GLuc activity was assessed using the same kit as for cell culture medium. For orthotopic tumors, animals were anesthetized and maintained with 2% isoflurane. A small incision (<1 cm) was made along the midline to expose the lower peritoneum, and the orthotopic tumor was located. MC complexes were then injected into 3–4 loci of each intraprostatic tumor (PC3MLN4, n = 10; LNCaP, n = 3), and then incisions were closed with sutures and staples. Tumor-free mice received equivalent injections of MC complexes into the anterior prostate lobe (n = 6). Urine samples were collected 1 day before and daily after MC injection for 7 days. To evaluate the cumulative secretion of GLuc into urine over the 7-day period, AUC analysis of GLuc activity measurements taken over time was performed.

In vivo therapeutic MC assessment in orthotopic tumors

Therapeutic MCs were prepared by combining pSurvivin-CD:UPRT-MCs (50 μ g/mouse) with 6 μ L *in vivo*-jetPEI to achieve an N/P ratio of 8 and injected intratumorally as described above for diagnostic MCs. Mice with PC3MLN4 FLuc+ orthotopic tumors were administered MC-PEI complexes (n = 9) or an equal volume of 0.9% saline as a control (n = 9). All animals received intraperitoneal injections of

500 mg/kg 5-FC diluted in 0.9% saline daily from days 1–7 post-injection and then every other day from days 7–14 post-injection. BLI was performed on days 0, 7, and 14 after MC-injection to assess cancer cell viability. BLI images were obtained using an automatic exposure time (max. 60 s) until peak signal was reached. Total tumor flux (p/s) at peak signal was quantified by manually placing regions of interest over the primary tumor.

Western blot analysis

Snap-frozen tumors were digested with radioimmunoprecipitation assay lysis buffer containing phosphatase inhibitors (Sigma). Protein concentrations were measured with a Pierce BCA protein assay (23227, Thermo Scientific, MA, USA). 50 µg of protein per sample was separated on 12% SDS-PAGE and then electro-blotted onto nitrocellulose membranes using the iBlot Dry Blotting System (Thermo Scientific). Membranes were blocked with 3% bovine serum albumin in PBS with 0.02% Tween 20 (PBST) for 1 h and then probed with rabbit anti-survivin antibody (1:10,000 dilution; Ab 76424, Abcam) at 4°C overnight (16 h). Following three washes with PBST, the membrane was incubated with IRDye 800CW goat anti-rabbit immunoglobulin G (IgG) (1:5,000 dilution, 925-32211, LI-COR Biosciences, NE, USA) for 1 h. Expression of GAPDH was used as a loading control using a mouse anti-GAPDH antibody (1:10,000 dilution, MAB374, Sigma) and IRDye 680CW goat anti-mouse IgG secondary antibody (1:5,000 dilution, 926-32220, LI-COR Biosciences). The fluorescent signal was measured using the Odyssey imaging system (LI-COR Biosciences). The same protocol was used to measure survivin levels in cell lysates.

Statistical analysis

All statistical analyses were performed in GraphPad Prism 8.0. Data were expressed as mean ± SD. For *in vitro* and *in vivo* studies, a Student's t test was used to measure differences between two groups, and a one-way ANOVA followed by Tukey's multiple comparisons test was used to compare means for more than two groups. When comparing multiple group means over time *in vivo*, a repeated-measures two-way ANOVA followed by Sidak's multiple comparisons test was used. For all tests, a nominal p value of less than 0.05 was deemed significant.

SUPPLEMENTAL INFORMATION

Supplemental Information can be found online at <https://doi.org/10.1016/j.omto.2021.01.007>.

ACKNOWLEDGMENTS

This work was funded in part by a Canada Graduate Master's Scholarship from the Natural Science and Engineering Research Council of Canada (to T.W.). This work was also funded by a Movember Discovery Grant (D2017-1970) from Prostate Cancer Canada (to J.A.R.) and the Petro Canada Young Innovator Award from Western University (to J.A.R.).

AUTHOR CONTRIBUTIONS

This work was supervised entirely by J.A.R. The study was designed by T.W. and J.A.R. Data acquisition and analysis were performed by T.W., D.G., and Y.C. The results were interpreted by T.W., Y.C.,

and J.A.R. The manuscript was prepared by T.W., A.L.A., and J.A.R. All authors edited, reviewed, and approved this submission.

DECLARATION OF INTERESTS

J.A.R. is co-inventor of a US patent called "Tumor-specific minicircles for cancer screening" (patent number 9534248; issued January 3, 2017), which describes the invention of survivin-driven minicircles encoding SEAP for cancer detection. This patent has been licensed by the start-up company Earli Inc., and J.A.R. holds shares and is a paid consultant of this company.

REFERENCES

- Bhang, H.E., and Pomper, M.G. (2012). Cancer imaging: Gene transcription-based imaging and therapeutic systems. *Int. J. Biochem. Cell Biol.* 44, 684–689.
- Kanerva, A., Zinn, K.R., Chaudhuri, T.R., Lam, J.T., Suzuki, K., Uil, T.G., Hakkarainen, T., Bauerschmitz, G.J., Wang, M., Liu, B., et al. (2003). Enhanced therapeutic efficacy for ovarian cancer with a serotype 3 receptor-targeted oncolytic adenovirus. *Mol. Ther.* 8, 449–458.
- Kaneko, S., Hallenbeck, P., Kotani, T., Nakabayashi, H., McGarrity, G., Tamaoki, T., Anderson, W.F., and Chiang, Y.L. (1995). Adenovirus-mediated gene therapy of hepatocellular carcinoma using cancer-specific gene expression. *Cancer Res.* 55, 5283–5287.
- Shah, K., Jacobs, A., Breakefield, X.O., and Weissleder, R. (2004). Molecular imaging of gene therapy for cancer. *Gene Ther.* 11, 1175–1187.
- Qiao, J., Doubrovin, M., Sauter, B.V., Huang, Y., Guo, Z.S., Balatoni, J., Akhurst, T., Blasberg, R.G., Tjuvajev, J.G., Chen, S.H., and Woo, S.L. (2002). Tumor-specific transcriptional targeting of suicide gene therapy. *Gene Ther.* 9, 168–175.
- Niu, G., and Chen, X. (2012). Molecular imaging with activatable reporter systems. *Theranostics* 2, 413–423.
- Bhang, H.E., Gabrielson, K.L., Laterra, J., Fisher, P.B., and Pomper, M.G. (2011). Tumor-specific imaging through progression elevated gene-3 promoter-driven gene expression. *Nat. Med.* 17, 123–129.
- Shah, K. (2005). Current advances in molecular imaging of gene and cell therapy for cancer. *Cancer Biol. Ther.* 4, 518–523.
- Ray, P., and De, A. (2012). Reporter gene imaging in therapy and diagnosis. *Theranostics* 2, 333–334.
- Eslami, M., Khamechian, T., Mazoochi, T., Ehteram, H., Sehat, M., and Alizargar, J. (2016). Evaluation of survivin expression in prostate specimens of patients with prostate adenocarcinoma and benign prostate hyperplasia underwent transurethral resection of the prostate or prostatectomy. *Springerplus* 5, 621.
- Mathieu, R., Lucca, I., Vartolomei, M.D., Mbeutcha, A., Klatte, T., Seitz, C., Karakiewicz, P.I., Fajkovic, H., Sun, M., Lotan, Y., et al. (2017). Role of survivin expression in predicting biochemical recurrence after radical prostatectomy: a multi-institutional study. *BJU Int.* 119, 234–238.
- Zhang, M., Coen, J.J., Suzuki, Y., Siedow, M.R., Niemierko, A., Khor, L.Y., Pollack, A., Zhang, Y., Zietman, A.L., Shipley, W.U., and Chakravarti, A. (2010). Survivin is a potential mediator of prostate cancer metastasis. *Int. J. Radiat. Oncol. Biol. Phys.* 78, 1095–1103.
- Richter, J.R., Mahoney, M., Warram, J.M., Samuel, S., and Zinn, K.R. (2014). A dual-reporter, diagnostic vector for prostate cancer detection and tumor imaging. *Gene Ther.* 21, 897–902.
- Garg, H., Salcedo, R., Trinchieri, G., and Blumenthal, R. (2010). Improved nonviral cancer suicide gene therapy using survivin promoter-driven mutant Bax. *Cancer Gene Ther.* 17, 155–163.
- Ahn, B.C., Ronald, J.A., Kim, Y.I., Katzenberg, R., Singh, A., Paulmurugan, R., Ray, S., Hofmann, L.V., and Gambhir, S.S. (2011). Potent, tumor-specific gene expression in an orthotopic hepatoma rat model using a Survivin-targeted, amplifiable adenoviral vector. *Gene Ther.* 18, 606–612.
- Shariat, S.F., Lotan, Y., Saboorian, H., Khoddami, S.M., Roehrborn, C.G., Slawin, K.M., and Ashfaq, R. (2004). Survivin expression is associated with features of biologically aggressive prostate carcinoma. *Cancer* 100, 751–757.

17. Chen, J.S., Liu, J.C., Shen, L., Rau, K.M., Kuo, H.P., Li, Y.M., Shi, D., Lee, Y.C., Chang, K.J., and Hung, M.C. (2004). Cancer-specific activation of the survivin promoter and its potential use in gene therapy. *Cancer Gene Ther.* *11*, 740–747.
18. Kay, M.A., Glorioso, J.C., and Naldini, L. (2001). Viral vectors for gene therapy: the art of turning infectious agents into vehicles of therapeutics. *Nat. Med.* *7*, 33–40.
19. Milone, M.C., and O'Doherty, U. (2018). Clinical use of lentiviral vectors. *Leukemia* *32*, 1529–1541.
20. Schirmbeck, R., Reimann, J., Kochanek, S., and Kreppel, F. (2008). The immunogenicity of adenovirus vectors limits the multispecificity of CD8 T-cell responses to vector-encoded transgenic antigens. *Mol. Ther.* *16*, 1609–1616.
21. Thomas, C.E., Ehrhardt, A., and Kay, M.A. (2003). Progress and problems with the use of viral vectors for gene therapy. *Nat. Rev. Genet.* *4*, 346–358.
22. Niidome, T., and Huang, L. (2002). Gene therapy progress and prospects: nonviral vectors. *Gene Ther.* *9*, 1647–1652.
23. Tan, Y., Li, S., Pitt, B.R., and Huang, L. (1999). The inhibitory role of CpG immunostimulatory motifs in cationic lipid vector-mediated transgene expression in vivo. *Hum. Gene Ther.* *10*, 2153–2161.
24. Marie, C., Vandermeulen, G., Quiviger, M., Richard, M., Pr at, V., and Scherman, D. (2010). pFARS, plasmids free of antibiotic resistance markers, display high-level transgene expression in muscle, skin and tumour cells. *J. Gene Med.* *12*, 323–332.
25. Darquet, A.M., Cameron, B., Wils, P., Scherman, D., and Crouzet, J. (1997). A new DNA vehicle for nonviral gene delivery: supercoiled minicircle. *Gene Ther.* *4*, 1341–1349.
26. Chen, Z.Y., He, C.Y., Ehrhardt, A., and Kay, M.A. (2003). Minicircle DNA vectors devoid of bacterial DNA result in persistent and high-level transgene expression in vivo. *Mol. Ther.* *8*, 495–500.
27. Chen, Z.Y., Riu, E., He, C.Y., Xu, H., and Kay, M.A. (2008). Silencing of episomal transgene expression in liver by plasmid bacterial backbone DNA is independent of CpG methylation. *Mol. Ther.* *16*, 548–556.
28. Ronald, J.A., Chuang, H.Y., Dragulescu-Andrasi, A., Hori, S.S., and Gambhir, S.S. (2015). Detecting cancers through tumor-activatable minicircles that lead to a detectable blood biomarker. *Proc. Natl. Acad. Sci. USA* *112*, 3068–3073.
29. Wang, T., Chen, Y., and Ronald, J.A. (2019). A novel approach for assessment of prostate cancer aggressiveness using survivin-driven tumour-activatable minicircles. *Gene Ther.* *26*, 177–186.
30. Malekshah, O.M., Chen, X., Noman, A., Sarkar, S., and Hatefi, A. (2016). Enzyme/Prodrug Systems for Cancer Gene Therapy. *Curr. Pharmacol. Rep.* *2*, 299–308.
31. Tannous, B.A., Kim, D.E., Fernandez, J.L., Weissleder, R., and Breakefield, X.O. (2005). Codon-optimized Gaussia luciferase cDNA for mammalian gene expression in culture and in vivo. *Mol. Ther.* *11*, 435–443.
32. Koyama, F., Sawada, H., Hirao, T., Fujii, H., Hamada, H., and Nakano, H. (2000). Combined suicide gene therapy for human colon cancer cells using adenovirus-mediated transfer of *Escherichia coli* cytosine deaminase gene and *Escherichia coli* uracil phosphoribosyltransferase gene with 5-fluorocytosine. *Cancer Gene Ther.* *7*, 1015–1022.
33. Tiraby, M., Cazaux, C., Baron, M., Drocourt, D., Reynes, J.P., and Tiraby, G. (1998). Concomitant expression of *E. coli* cytosine deaminase and uracil phosphoribosyltransferase improves the cytotoxicity of 5-fluorocytosine. *FEMS Microbiol. Lett.* *167*, 41–49.
34. Miyagi, T., Koshida, K., Hori, O., Konaka, H., Katoh, H., Kitagawa, Y., Mizokami, A., Egawa, M., Ogawa, S., Hamada, H., and Namiki, M. (2003). Gene therapy for prostate cancer using the cytosine deaminase/uracil phosphoribosyltransferase suicide system. *J. Gene Med.* *5*, 30–37.
35. Vickers, A.J., and Brewster, S.F. (2012). PSA Velocity and Doubling Time in Diagnosis and Prognosis of Prostate Cancer. *Br. J. Med. Surg. Urol.* *5*, 162–168.
36. Kwong, G.A., Dudani, J.S., Carrodegua, E., Mazumdar, E.V., Zekavat, S.M., and Bhatia, S.N. (2015). Mathematical framework for activity-based cancer biomarkers. *Proc. Natl. Acad. Sci. USA* *112*, 12627–12632.
37. Kim, T.K., and Eberwine, J.H. (2010). Mammalian cell transfection: the present and the future. *Anal. Bioanal. Chem.* *397*, 3173–3178.
38. Zimmermann, J.S., Osieka, R., Bruns, T., Hollberg, H., Wiechmann, B., Netzbandt, O., Sablotny, J., Malade, M., Heitz, M., Bernhardt, F., et al. (2018). Five-year effectiveness of low-dose-rate brachytherapy: comparisons with nomogram predictions in patients with non-metastatic prostate cancer presenting significant control of intra- and periprostatic disease. *J. Contemp. Brachytherapy* *10*, 297–305.
39. Bhatnagar, A., Wang, Y., Mease, R.C., Gabrielson, M., Sysa, P., Minn, I., Green, G., Simmons, B., Gabrielson, K., Sarkar, S., et al. (2014). AEG-1 promoter-mediated imaging of prostate cancer. *Cancer Res.* *74*, 5772–5781.
40. Ikegami, S., Tadakuma, T., Ono, T., Suzuki, S., Yoshimura, I., Asano, T., and Hayakawa, M. (2004). Treatment efficiency of a suicide gene therapy using prostate-specific membrane antigen promoter/enhancer in a castrated mouse model of prostate cancer. *Cancer Sci.* *95*, 367–370.
41. Jaiswal, P.K., Goel, A., and Mittal, R.D. (2015). Survivin: A molecular biomarker in cancer. *Indian J. Med. Res.* *141*, 389–397.
42. Figueiredo, M.L., Sato, M., Johnson, M., and Wu, L. (2006). Specific targeting of gene therapy to prostate cancer using a two-step transcriptional amplification system. *Future Oncol.* *2*, 391–406.
43. Iyer, M., Wu, L., Carey, M., Wang, Y., Smallwood, A., and Gambhir, S.S. (2001). Two-step transcriptional amplification as a method for imaging reporter gene expression using weak promoters. *Proc. Natl. Acad. Sci. USA* *98*, 14595–14600.
44. Schaarschmidt, D., Baltin, J., Stehle, I.M., Lipps, H.J., and Knippers, R. (2004). An episomal mammalian replicon: sequence-independent binding of the origin recognition complex. *EMBO J.* *23*, 191–201.
45. Ronald, J.A., Cusso, L., Chuang, H.Y., Yan, X., Dragulescu-Andrasi, A., and Gambhir, S.S. (2013). Development and validation of non-integrative, self-limited, and replicating minicircles for safe reporter gene imaging of cell-based therapies. *PLoS ONE* *8*, e73138.
46. Zhang, H.K., Chen, Y., Kang, J., Lisok, A., Minn, I., Pomper, M.G., and Bector, E.M. (2018). Prostate-specific membrane antigen-targeted photoacoustic imaging of prostate cancer in vivo. *J. Biophotonics* *11*, e201800021.
47. Liu, M.A., and Ulmer, J.B. (2005). Human clinical trials of plasmid DNA vaccines. *Adv. Genet.* *55*, 25–40.
48. Chen, Z.Y., He, C.Y., Meuse, L., and Kay, M.A. (2004). Silencing of episomal transgene expression by plasmid bacterial DNA elements in vivo. *Gene Ther.* *11*, 856–864.
49. Catanese, D.J., Jr., Fogg, J.M., Schrock, D.E., 2nd, Gilbert, B.E., and Zechiedrich, L. (2012). Supercoiled Minivector DNA resists shear forces associated with gene therapy delivery. *Gene Ther.* *19*, 94–100.
50. Stenler, S., Wiklander, O.P., Badal-Tejedor, M., Turunen, J., Nordin, J.Z., Halleng ard, D., Wahren, B., Andaloussi, S.E., Rutland, M.W., Smith, C.I., et al. (2014). Micro-minicircle Gene Therapy: Implications of Size on Fermentation, Complexation, Shearing Resistance, and Expression. *Mol. Ther. Nucleic Acids* *2*, e140.
51. Zhao, N., Fogg, J.M., Zechiedrich, L., and Zu, Y. (2011). Transfection of shRNA-encoding Minivector DNA of a few hundred base pairs to regulate gene expression in lymphoma cells. *Gene Ther.* *18*, 220–224.
52. Chuang, Y.C., Chiang, P.H., Huang, C.C., Yoshimura, N., and Chancellor, M.B. (2005). Botulinum toxin type A improves benign prostatic hyperplasia symptoms in patients with small prostates. *Urology* *66*, 775–779.
53. Nasu, Y., Saika, T., Ebara, S., Kusaka, N., Kaku, H., Abarzua, F., Manabe, D., Thompson, T.C., and Kumon, H. (2007). Suicide gene therapy with adenoviral delivery of HSV-tK gene for patients with local recurrence of prostate cancer after hormonal therapy. *Mol. Ther.* *15*, 834–840.
54. Chen, Z., Penet, M.F., Krishnamachary, B., Banerjee, S.R., Pomper, M.G., and Bhujwalla, Z.M. (2016). PSMA-specific theranostic nanoplex for combination of TRAIL gene and 5-FC prodrug therapy of prostate cancer. *Biomaterials* *80*, 57–67.
55. Chen, Z., Penet, M.F., Nimmagadda, S., Li, C., Banerjee, S.R., Winnard, P.T., Jr., Artemov, D., Glunde, K., Pomper, M.G., and Bhujwalla, Z.M. (2012). PSMA-targeted theranostic nanoplex for prostate cancer therapy. *ACS Nano* *6*, 7752–7762.
56. Kay, M.A., He, C.Y., and Chen, Z.Y. (2010). A robust system for production of minicircle DNA vectors. *Nat. Biotechnol.* *28*, 1287–1289.
57. Euhus, D.M., Hudd, C., LaRegina, M.C., and Johnson, F.E. (1986). Tumor measurement in the nude mouse. *J. Surg. Oncol.* *31*, 229–234.
58. Cunningham, D., and You, Z. (2015). In vitro and in vivo model systems used in prostate cancer research. *J. Biol. Methods* *2*, 2.